14

Edge detection in microscope images

M. Y. JAISIMHA and R. M. HARALICK

Introduction

One of the central problems in biological and biomedical imaging in general, and in cytological imaging in particular, is the automatic determination of the boundaries of objects of interest. The problem of edge detection in cytological images is further compounded by the wide variety of images that can be obtained. In addition, the greylevel characteristics of the extraneous objects in the images are often very similar to those of the objects of interest. If no prior knowledge is available about the nature of the image, it is then necessary to analyse the greylevel characteristics of the objects of interest, the extraneous objects and the background adjacent to the boundaries of interest. These factors have to be taken into account in order to design a successful image analysis procedure. As we show in this chapter, it is sometimes impossible to perform the desired delineation purely on the basis of domain-independent greylevel spatial information. Some cytological knowledge may have to be incorporated to perform good edge detection.

A large number of image analysis tools are available to the researcher in order to perform an analysis of the greylevel and shape properties of an image. Many of these tools were first developed for machine vision applications and some were developed for cytological image analysis. A judicious combination of some of these procedures can be used for analysing cytological images. Expositions on the vast body of image analysis procedures can be found in Haralick & Shapiro (1991) and in Rosenfeld & Kak (1982). In this chapter, we review briefly the most significant tools used in edge detection in cytological images.

Applying a pure edge detection procedure, such as the facet edge detector (Haralick, 1984) or the Prewitt detector (Prewitt, 1970), to a cytological image directly can have disastrous consequences in terms of the quality of the boundaries detected. A general approach is to apply iterations of conditioning and labelling to the images. Conditioning is based on a model suggesting that the observed image is composed of an informative pattern modified by uninteresting variations that typically add to or multiply the informative pattern.

Conditioning estimates the informative pattern on the basis of the observed image. Thus conditioning suppresses noise, which can be thought of as random unpatterned variations affecting all measurements. Conditioning can also perform background normalization by suppressing uninteresting systematic or patterned variations. Conditioning is typically applied uniformly and is context independent.

Labelling is based on a model that suggests that the informative pattern has structure as a spatial arrangement of events, each spatial event being a set of connected pixels. Labelling determines the kinds of spatial events each pixel participates in. For example, if the interesting spatial events of the informative pattern are events only of high valued and low valued pixels, then the thresholding operation can be considered a labelling operation. Other kinds of labelling operations include edge detection, corner finding, and identification of pixels that participate in various shape primitives. Mathematical morphology is used in both the conditioning and labelling phases of the algorithms.

Thresholding is a process of labelling a greylevel image on the basis of the greylevel value. Thresholding transforms a greylevel image into a binary image. Once an image has been thresholded, the binary image can be analysed to identify the various distinct, yet connected, entities that make it up. The process of identifying connected entities in a binary image is referred to as connected components analysis. The basic theory behind thresholding and connected components analysis is presented in the next section. Before thresholding or other edge detection procedures can be applied to an image, the image has to be conditioned to mitigate the effects of noise or extraneous objects. After thresholding, the shape properties of the objects have to be analysed. The tools of mathematical morphology can be used to perform these tasks and a somewhat qualitative introduction to this subject is given in a section below. A brief introduction to the facet model and edge detection based on this model is also provided.

Some objects of interest in cytological images have a boundary that is composed of components with fairly distinct greylevel characteristics. It is also possible for some edge detection procedures to perform relatively well in detecting certain components of the boundaries without being able to detect all of them. An obvious step is to use the results of each edge detection procedure where it works best. The procedures we describe in this chapter employ this principle. We present procedures that use a combination of thresholding, morphology, facet model-based edge detection and region property analysis for edge detection in four different cytological images.

Thresholding and connected components

Thresholding is the process of labelling the pixels in a greylevel image based on their greylevel values. It has been used extensively as a first step in binary machine vision. Thresholding can be used to distinguish pixels that have a

lower greylevel value from those having a higher greylevel value. Pixels having a value higher than the threshold value are associated with one label (say a binary 1) and those lower than the threshold value are associated with another label (typically a binary 0).

Procedures exist for automatically determining the threshold based on the histogram of the pixels in the image (Haralick & Shapiro, 1991). If the objects of interest occupy a significant fraction of the image and have a greylevel value sufficiently different from the background, the greylevel histogram that results is bimodal with a fairly deep valley between the two modes. Automatic thresholding procedures attempt to identify this valley and place the threshold value at this location. Unfortunately, in cytological images the objects of interest quite often satisfy neither of the two assumptions that automatic procedures depend on for their functioning. Threshold selection thus has to be done manually. This is not unduly restrictive in practice since the threshold value depends to a large extent on a knowledge of the nature of the image. A complete system for cell image segmentation would require *a priori* knowledge to determine the threshold value.

Once the image has been thresholded, a connected components operator (Lumia *et al.*, 1983) can be used to group the binary 1 pixels into maximally connected regions which are referred to as connected components. Two pixels are said to be connected if there is a path between them lying entirely on binary 1 pixels and where each pixel on the path is connected to one of its binary 1 neighbours. If the path is restricted to turns in the four cardinal compass directions (north, south, east and west), the pixels are said to be 4-connected. If the intermediate compass directions are allowed, the pixels are called 8-connected. A thresholded image is used as input to the connected components algorithm and the output consists of a symbolic image where the label assigned to each pixel is an integer that uniquely identifies the connected component on which the pixel lies. Once the connected component image has been generated, the region properties can be computed. A full description of these properties is given in Haralick & Shapiro (1991). In this chapter, the following properties are used to distinguish between the various components and perform edge detection:

1 The mean and variance of the greylevel value of the pixels that contribute to a given component.
2 The size of the component.
3 The circularity measure of the component.

Mathematical morphology

Mathematical morphology is a powerful algebraic system of operators which has been extensively used in shape analysis (Haralick & Shapiro, 1991; Giardina & Dougherty, 1988; Haralick *et al.*, 1987). Using the basic morphological operators of dilation, erosion, opening and closing (defined below),

shape primitives can be extracted from images and contaminating structures discarded. The contaminating structures could either be random noise or shapes with characteristics that differ from those of the shapes of interest. In a typical morphological image processing algorithm the image is operated on by a relatively small kernel or structuring element which is selected to achieve the intended effect.

Dilation, as the name implies, results in expansion or swelling of the image. In set notation, the dilation of the two sets A and B is denoted by $A \oplus B$ and is defined as:

$$A \oplus B = \{c \in E^N | c = a + b \text{ for some } a \in A \text{ and } b \in B\}$$

The above definition holds for binary (two level) images that might, for example, be obtained from the output of a thresholding operation.

Erosion results in a contraction of the image. In set notation, the erosion of the two sets A and B is denoted by $A \ominus B$ and is defined as:

$$A \ominus B = \{x \in E^N | x + b \in A \text{ for every } b \in B\}$$

The opening of two sets A and B can be defined in terms of the dilation and erosion operators as follows:

$$A \bigcirc B = (A \ominus B) \oplus B$$

The closing of two sets is defined as:

$$A \bullet B = (A \oplus B) \ominus B.$$

Binary openings can be used to eliminate additive noise in the background and closings can be used to eliminate subtractive noise in the foreground of binary images. In the case of greylevel images, the definition of the dilation (erosion) operator is modified in terms of maxima (minima) of sums (differences) of the structuring element and image greylevel values in the domain of the structuring elements. Greylevel closings can be used to fill 'dark pits' and greylevel openings can be used to eliminate 'bright hills' in images. A complete introduction to the theory and applications of mathematical morphology can be found in the studies of Giardina & Dougherty (1988), Haralick & Shapiro (1991), Haralick *et al.* (1987) and Costa (1990).

The facet model

A common strategy for edge detection in the machine vision literature has been to model edges in the images as being derived from a step change (or blurred versions of a step) in the greylevel value. Pixels are then labelled as edge pixels if the change in greylevel value, or the gradient, is high enough. A gradient magnitude edge detector that can be used is the second directional derivative edge detector described by Haralick (1984) and Haralick & Shapiro (1991). The edge detector uses the facet model to estimate the gradient magnitude at each pixel location in the image. The facet model considers a digital image as being derived by sampling a continuous underlying greylevel intensity surface.

Each neighbourhood of this surface can be represented by a low degree polynomial, usually quadratic or cubic. In the cubic case, the polynomial or 'facet' is:

$$f(r,c) =$$
$$k_1 + k_2 r + k_3 c + k_4 r^2 + k_5 rc + k_6 c^2 + k_7 r^3 + k_8 r^2 c + k_9 r c^2 + k_{10} c^3,$$

where k_i are the polynomial coefficients,
r are the row co-ordinates and
c are the column coordinates.

The first step in the edge detection sequence is the computation of the polynomial coefficients by performing a local surface fit over a neighbourhood centred around each pixel in the image. The coefficients $\{a_i\}$ are computed by minimising:

$$e^2 = \sum_{r \in R} \sum_{c \in C} [I(r,c) - \sum_{n=0}^{K} a_n P_n(r,c)],$$

where R and C are the set of row and column coordinates respectively that belong to the neighbourhood,
$I(r,c)$ is the pixel intensity at coordinate (r,c) and
$P_n(r,c)$ is the set of Chebyshev polynomials, used as basis polynomials.

The gradient direction is given in terms of the polynomial coefficients as $\arctan(k_3/k_2)$ and the gradient magnitude is given by $(k_2^2 + k_3^2)^{1/2}$. The second directional derivative in the direction of the gradient and the contrast can also be obtained in terms of the facet polynomial coefficients (Haralick, 1984).

The centre pixel of the neighbourhood is labelled as an edge pixel if the second directional derivative in the direction of the gradient has a negatively sloped zero crossing within a threshold radius of the centre of the pixel and if the edge contrast exceeds a threshold value. That is, an edge is detected at (r,c) if:

1 $f'(r,c) \neq 0$
2 $f''(x,y) = 0$ for some (x,y) within a threshold radius of (r,c)
3 $f'''(x,y) < 0$

where f', f'' and f''' denote the first, second and third directional derivatives of the facet polynomial. Increasing the size of the window permits the detection of relatively flat-sloped edges. Increasing the degree of the polynomial approximation to the image neighbourhood improves the ability of the detector to detect relatively sharp edges.

Boundary detection in cell images

Boundary detection and/or segmentation of cell images is usually the first step in an image understanding system where a high level module utilizes the output

of a low level boundary extraction and region characterization procedure to perform quantitative and qualitative measurements. Boundaries in cell images are usually of two types:

1 Boundaries of relatively small spatial extent characterized by 'cliffs' between regions of different greylevel intensity, similar to the 'frontier' boundaries described by Garbay (1986).
2 Boundaries of relatively large spatial extent are characterized by a particular greylevel intensity or intensity pattern. That is, there are 'moats' that are characterized by regions of relatively lower greylevel intensity and 'walls' that are characterized by relatively higher greylevel intensities.

Gradient based edge detectors and region growing operators can be used to identify cliff boundaries. Moat and wall boundaries can be identified either by thresholding or gradient based edge operators. In most cases, the boundaries in real cell images are not perfect cliffs, moats or walls. In addition to noise in the images, there are also extraneous objects whose boundary characteristics are indistinguishable from the objects of interest (whose boundaries are to be identified). In addition, there may be objects that touch and hence have to be grouped together in the boundary delineation step.

In order to contend with the problems of real cell images, conditioning operators may have to be applied to attenuate the effects of noise or to remove regular patterned variations in the background which could produce spurious boundaries. Boundary identification can be performed by iterations of labelling with facet edge detection, thresholding or region growing, interspersed with conditioning iterations. Connected component analysis with region property computation can also be used to differentiate between spurious and legitimate boundaries. Where the boundaries of the objects of interest are combinations of the various kinds of boundaries, the outputs of various edge detection schemes can be combined to yield the desired output.

Algorithms for edge detection in microscopic images

Algorithms and results for edge detection in four different images, from both conventional and confocal microscopes, are presented below. For three of the four images, 'ideal' edge boundaries were identified by an expert. Procedures were designed that produced an edge output that was as close as possible to the 'ideal'. For each image, the features were identified that determined the design of an image analysis procedure. The analysis procedure and the results obtained with it are described below. Lastly, the overall algorithms are presented in a compact mathematical notation. The notation used is derived from that of Joo (1991).

At each sub-step i, G^i or B^i denotes the greylevel or binary image obtained

as a result of step i. Step i operates on the output of step $i-1$. The first step operates on G^0, the input greylevel image. To reiterate, the morphological operators are defined as follows:

- $\oplus$ denotes dilation
- $\ominus$ denotes erosion
- $\bigcirc$ denotes opening
- $\bullet$ denotes closing.

Structuring elements for morphological operations are defined as follows:

1. *disc*(r) denotes a digital disc of radius r with the structuring element centred at the origin.
2. *horizline*(l) denotes a horizontal line of length l with the structuring element origin at (0,0).

Thresholding operators are defined by the symbols $>$ or $\leqslant$ where:

$$B^i = G^{i-1} \leqslant t$$

denotes the process of thresholding such that all pixels in G^{i-1} less than the threshold value t are set to a binary 0. Where the thresholding is performed relative to the running row mean, the threshold is expressed as $\bar{x}$, where x times the running row mean is used as a threshold.

1. The inversion of a binary image B^i is denoted by $\bar{B}^i$.
2. The intersection ($\cap$) of two binary images B^i and B^{i-1} is denoted by $B^i \cap B^{i-1}$.
3. The union ($\cup$) of two binary images is denoted by $B^i \cup B^{i-1}$.
4. The set difference operator is denoted by $-$.
5. C^i denotes the connected component image and the associated greylevel and component properties obtained as a result of a connected component and region property computation at step i.
6. The connected component operation on a binary image B^{i-1} is denoted by $C^i = conn(B^{i-1})$.
7. $size(C^i) < t$ denotes the operation of deleting all components from C^i whose size is less than t.
8. $max(C^i)$ denotes the largest connected component in C^i.
9. $mg(C^i) < t$ denotes the operation of deleting all components from C^i whose mean greylevel is less than t.
10. $circul(C^i) \geqslant t$ denotes the operation of deleting all connected components from C^i whose circularity measure is greater than t.
11. Facet edge detection on the image G^i is represented by the function $fedg(G^i,o,s,e,r)$ where o is the order of the facet fit (cubic for example), s is the size of each side of the window of the facet fit, e is the edge contrast threshold and r is the radius threshold for the zero crossing of the second directional derivative edge detector. The resulting edge image has binary 1 pixels at all edge locations.

12 The function $mark(B^i)$ denotes the process of marking the boundary pixels of the binary image B^i.

13 The function $rgg(G^i, B^i, s)$ denotes the process of performing a greylevel based, region growing operation on the image G^i where the regions are constrained to lie within the edges defined by the binary image B^i (with the edge pixels having a binary 1 value). s is the significance level of the test for growing regions. The region growing scheme (Haralick & Shapiro, 1991) first performs a top–down, left–right scan where neighbouring regions/pixels are compared for equality of pixel value and region mean using a t-statistic test. Regions with sufficiently low t-values are merged. Multiple top–down and bottom–up merging scans are also performed. Greylevel properties for each of the regions are also computed. The output of the region grower is denoted by R^i.

14 The function $merge(R^i)$ merges all adjacent regions and produces a binary image.

Image 1

The first example image was from a confocal scanning laser microscope. It consists of adult human respiratory mucosa stained with an indirect immunofluorescence method to reveal the nerves. The image is shown in Fig. 1. The nerves appear in white. The large object in the centre of the image is a nerve bundle. Above the nerve bundle is a large cavernous blood vessel. In this image all nerves are of interest. The ideal boundaries of the nerves were not available.

The edge contrast is high, and the extraneous objects have a much lower greylevel value than the objects of interest. The boundaries of the objects of interest are of the type 'cliff'. The images have a gradation in the background greylevel which can cause problems if a single threshold value is used for the entire image. The solution to this problem is to use a threshold that depends on the local mean greylevel value. The exact threshold value $t(r)$ for row r of the image is given by the running mean:

$$t(r) = x \times \frac{1}{N_{\text{COLS}} \times 20} \times \sum_{i=r-10}^{r+10} \sum_{j=1}^{N_{\text{COLS}}} I(r,c)$$

where x is a user defined control factor,

N_{COLS} is the number of pixels per row of the image,

c is the column number of the pixel and

$I(r,c)$ is the image greylevel at location (r,c).

The actual value of x used for the image was 2.1 (step 1). The output of the thresholding step is subject to a connected components analysis. All connected components whose size is less than 25 pixels (step 2) (smaller than the smallest nerve) and mean greylevel value less than 110 (darker than the darkest nerve) (step 3) are discarded to yield the final image (step 5).

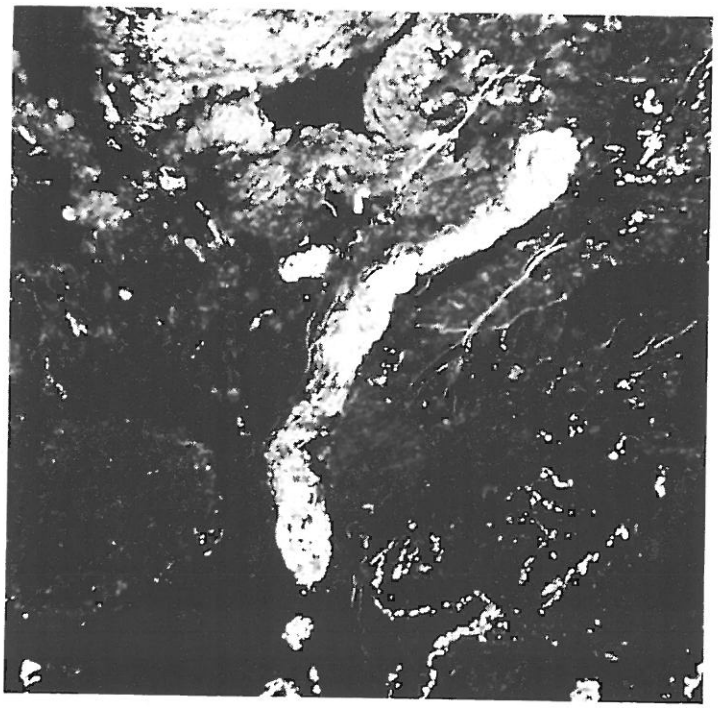

Fig. 1. Image 1. Confocal microscope image of adult respiratory mucosa stained with an indirect immunofluorescence method to reveal the nerves (white).

The overall algorithm is as follows:

1 $B^1 = G^0 < 2.1$
2 $C^2 = conn(B^1)$
3 $C^3 = size(C^2) < 25$
4 $C^4 = mg(C^3) < 110$
5 $B^5 = C^4 \leqslant 0$

The output of the procedure is shown in Fig. 2.

Image 2

The second example image was obtained from a television camera and is an image of a radial diffusion agarose gel. The objects traced in Fig. 3 are the precipitations of interest. The objects of interest have only their outer outlines marked as being relevant. The image has the following characteristics which have to be taken into account in the image analysis procedure:

1 There is random noise in the image.
2 There is a non-uniform background greylevel.
3 All objects have a bright spot at the centre.

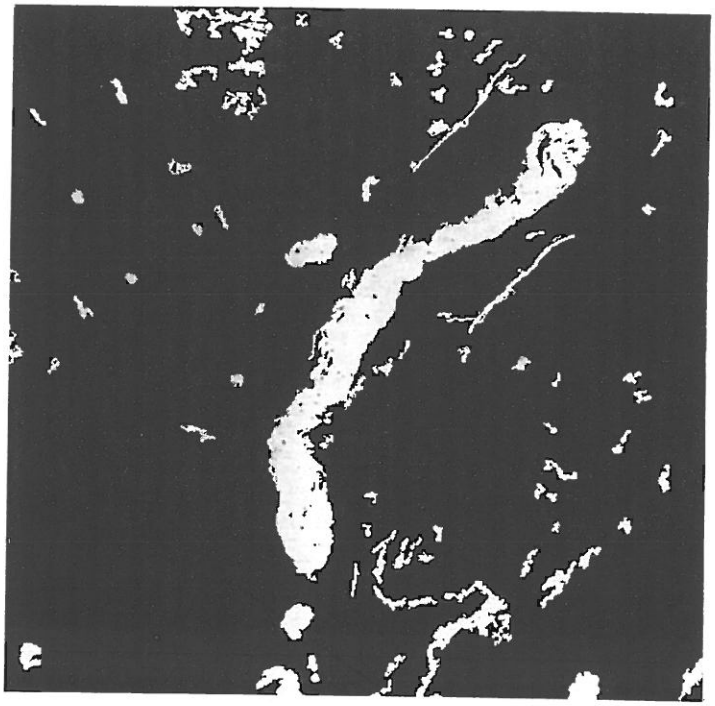

Fig. 2. Image 1. Result of edge detection procedure.

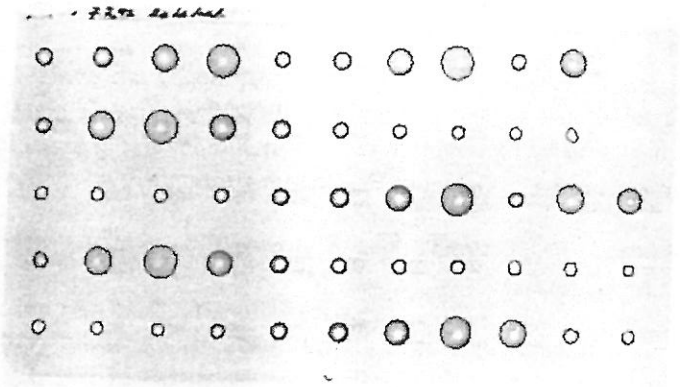

Fig. 3. Image 2. Television camera image of a radial diffusion agarose gel.

4 The only objects of interest are those that have some darkening around the boundary (corresponding to the precipitation of interest).

The precipitation results in a moat region between the bright interior and the bright background. However, since only the outer boundary of the moat is of interest, the moat has first to be converted into a boundary of the type cliff. This is achieved by the first step of conditioning the image, which is to perform a greyscale opening of the image (step 1) with a horizontal line whose extent is slightly larger than the radius of the largest bright spot on the object. The line segment used is of size 15 pixels. The greyscale opening retains all objects with a significant amount of precipitation. However, a few of the objects which have only a small amount of precipitation are merged with the background.

The image obtained from the opening is subject to facet edge detection using a cubic facet with a 5×5 window and an edge contrast threshold of 12.0 (step 2). This produces the boundaries of all the objects which were preserved after the opening. The appropriate algorithm to detect the objects which were missed by the facet edge detector is now applied. The original image is first thresholded with a threshold of 155 (step 3). The threshold is high enough to detect the bright centres of all the objects. All the bright centres that were detected by the facet edge detector now have to be masked out. The image obtained after the initial conditioning by opening is now thresholded at a value (136) such that all objects that have a sufficient contrast (and were hence picked up by the facet edge detector) are detected (step 4). The labelled image from this thresholding is now subject to iterations of conditioning with morphological opening with a disc of radius 3 pixels (to eliminate small additive noise 'blobs' in the foreground) (step 5) and closing with a disc of radius 3 (to reconnect any blobs that were split into two by the opening) (step 6).

The image is then inverted (step 7) and used as a mask on the image (step 8) obtained from step 3 to remove the blobs corresponding to boundaries detected by the facet edge detector. The remaining blobs are dilated by a disc of radius 3 and the boundaries of the dilated blobs are marked (step 9). This yields the boundaries of all the bright objects not detected by the facet edge detector. Only those objects with some precipitation are to be detected. In order to do so, a connected-components analysis is performed on the boundary image (step 10). The means of the greylevels of pixels underlying the boundaries on the original greylevel image were also computed. All boundaries whose mean greylevel values exceed 151 (step 11) were then discarded. This yields the set of all boundaries of interest not detected by the facet edge detector. The two images generated by the facet edge detector and the connected component analysis procedure are then combined (through a logical ⟨OR⟩ operation: step 12) to yield the final edge image which is shown in Fig. 4. It can be seen that some false alarms exist in the final output in terms of spurious boundaries that do not correspond to the boundary of any of the objects of interest and the boundary of the slide on which the precipitations were generated is also detected. However, a post-processing module which analyses the output of the

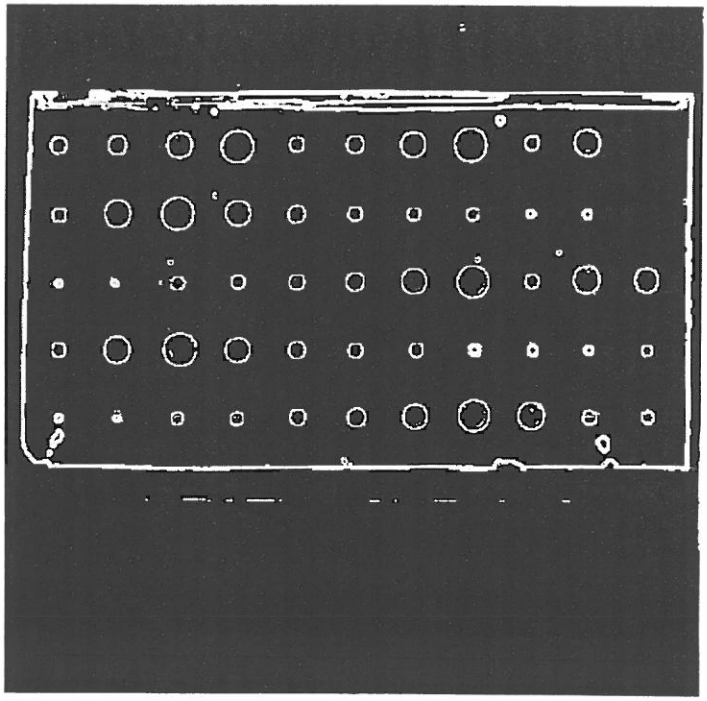

Fig. 4. Image 2. Result of edge detection procedure.

edge detection module could use the knowledge of the relative position of the slide in the frame and the fact that the precipitation centres are located on a square grid on the slide to discard these false alarms. An important aspect of the edge delineation problem was to detect only the outer dark edges of objects corresponding to some precipitation. The algorithm described in this section is able to perform the required edge detection. In mathematical notation the algorithm is as follows:

1 $G^1 = G^0 \bigcirc horizline(15)$
2 $B^2 = fedg(G^i, 3, 5, 12.00, 0.7)$
3 $B^3 = G^0 \leqslant 155$
4 $B^4 = G^1 \geqslant 136$
5 $B^5 = B^4 \bigcirc disc(3)$
6 $B^6 = B^5 \bullet disc(3)$
7 $B^7 = \bar{B}^6$
8 $B^8 = B^3 \cup B^7$
9 $B^9 = mark(B^8 \oplus disc(3))$
10 $C^{10} = conn(B^9)$
11 $C^{11} = mg(C^{10}) > 151$
12 $B^{12} = (C^{11} \leqslant 0) \cup B^2$

The final output of the detection procedure is shown in Fig. 4.

Image 3

The third example image was generated from a light microscope and is an image of adult guineapig lung tissue stained with haematoxylin and eosin. The image is shown in Fig. 5. The boundary of interest is shown traced on the image. The structure traced is an airway. The pulmonary artery is situated to the left of the airway. The structure of interest in the image is fairly well defined in its geometry and is also substantially darker in greylevel than any of the other structures in the image. The boundary structure of interest is clearly a moat because of the characteristics just mentioned. An obvious first step is to start by labelling all pixels whose greylevel value is equal to or less than that of the brightest pixels in the airway of interest (step 1). The threshold value is chosen as 136. This yields a large number of small structures, apart from the airway of interest, which are clutter.

The labelled image now has to be conditioned to eliminate clutter. Once again iterations of morphological operations can be used – first opening with a disc of radius 9 (to remove the small structures) (step 2) and then closing the output of the opening of step 2 with a disc of radius 15 (to reconnect the small segments into which the airway of interest has been broken: step 3). A consequence of the opening iteration is that the airway of interest is now split into two large pieces and a number of relatively small clutter objects remain in

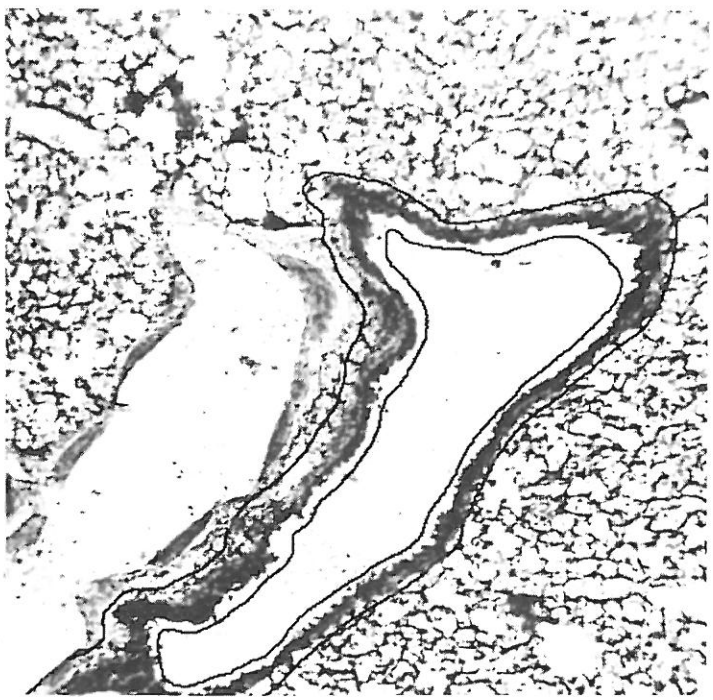

Fig. 5. Image 3. Conventional microscope image of adult guineapig lung tissue stained with haematoxylin and eosin.

the background. Next a connected components analysis is performed on the output of the closing and all but the two largest components are discarded (step 5). The two large components are then joined together by closing with a large disc of radius 25. The single structure is then dilated by a disc of radius 7 (step 6) before obtaining the final boundary (step 7). The boundary is shown in Fig. 6. The dark airway of interest is delineated as needed. The edge detection in this image is more straight forward than for Image 2 because of the distinct geometry and greylevel characteristics of the airway of interest. The overall detection algorithm is as follows:

1 $B^1 = G^0 \geqslant 136$
2 $B^2 = B^1 \bigcirc disc(9)$
3 $B^3 = B^2 \bullet disc(15)$
4 $C^4 = conn(B^3)$
5 $C^5 = max(C^4) \cap max(C^4 - (max(C^4)))$
6 $B^6 = (C^5 \leqslant 0) \oplus disc\ 7$
7 $B^7 = mark(B^6)$

The final output of the edge detector is shown in Fig. 6.

Image 4

The fourth example image was from a light microscope. The section was of adult human respiratory mucosa stained with haematoxylin and eosin. The

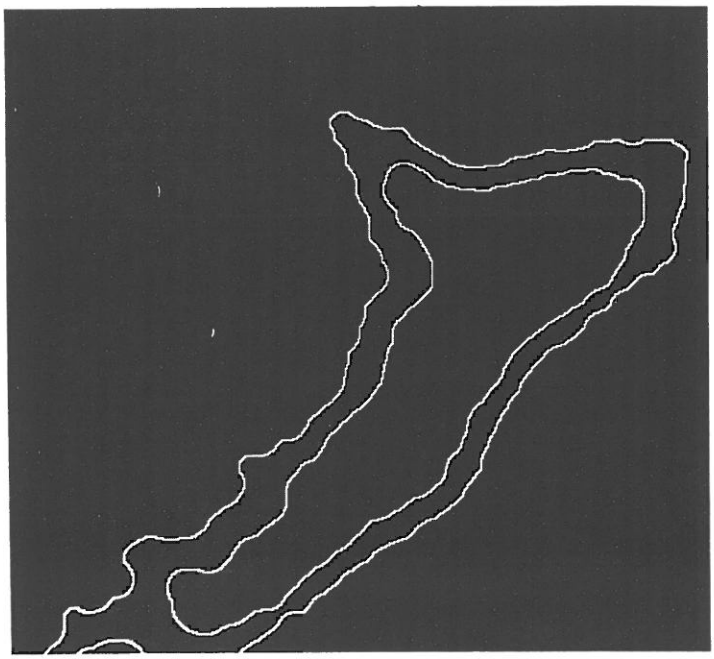

Fig. 6. Image 3. Result of edge detection procedure.

image is shown in Fig. 7, with the boundaries of interest shown traced over the greylevel image. The traced structures are the large cavernous blood vessels. Of the four example images, this one best illustrates the factors an image analysis researcher must cope with in segmenting cell images. The delineated objects of interest and large portions of the background have the same brightness (in terms of greylevel value). The boundaries of the delineated objects (with one exception) have the following characteristics:

1 Portions of the boundaries have a small greylevel contrast with the background – they are cliff boundaries.
2 Other portions of the boundaries have a greylevel 'shadow', i.e. the greylevel value immediately adjacent to the boundary of the object is substantially lower than the greylevel value of either the object or the background adjacent to the boundary – these boundary regions can be considered to be shallow moats.

The one exception is the U-shaped object at the centre of the image in Fig. 7 which has a region at the centre of the object that has greylevel characteristics identical with the boundaries of all the other objects in the scene! This poses problems for the edge detection procedure. In addition, there are extraneous objects in the background that have greylevel characteristics identical with

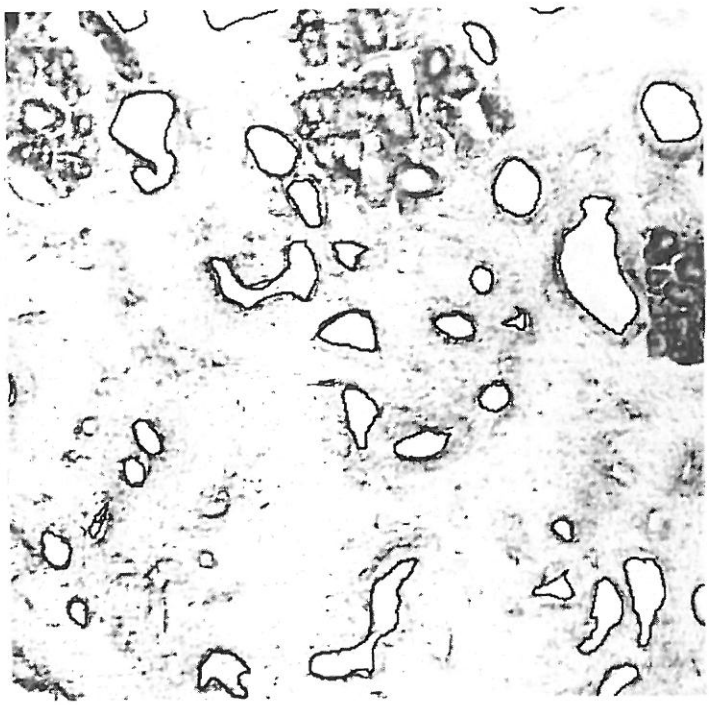

Fig. 7. Image 4. Conventional microscope image of adult human respiratory mucosa stained with haematoxylin and eosin.

those of the objects of interest. The background also has numerous small dark 'pits' which have to eliminated as far as possible in the initial conditioning phase.

As a first step of the algorithm, the image is closed with a disc of radius 5 (step 1). As mentioned in the section on morphology, greylevel closings have the property of being able to fill 'pits'. The output of the closing is subject to facet edge detection (step 2). A cubic facet is used with a 9×9 window and an edge contrast threshold of 10. The edge image obtained is shown in Fig. 8. Clearly, the output of the edge detector has a large number of spurious boundaries in the background of the image. This edge detection strategy, however does a good job of selecting the portions of the boundary corresponding to contrast variations while at the same time preserving the connectivity of the U-shaped object. In order to detect the portions of the boundary that correspond to the 'shadow' regions, another labelling step is performed, thresholding the closed image with a threshold value (of 115) approximately equal to the greylevel value of the 'shadow' regions (step 3). This produces the image of Fig. 9. In order to discard the spurious edge boundaries and to use the greylevel statistics of the objects of interest, a region growing scheme is used (Haralick & Shapiro, 1991) that operates on the greylevel image. The region grower is restricted to growing regions that lie within the boundaries detected by the thresholding and facet edge detection schemes. The output of the region

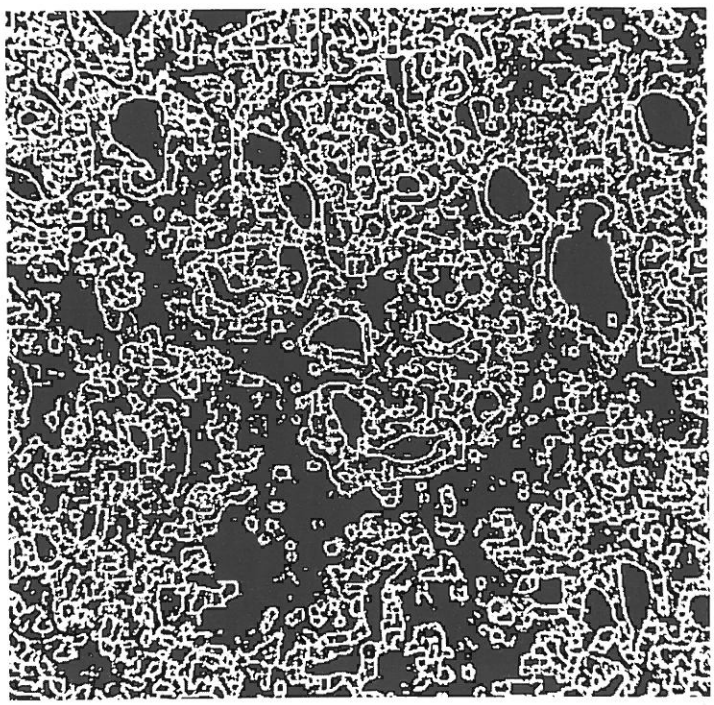

Fig. 8. Image 4. Result of facet edge detector.

Fig. 9. Image 4. Result of thresholding procedure at a threshold of 115.

grower is subject to connected components analysis and the greylevel properties of the image underlying each of the components are also computed (step 4). All components from the output of the region grower are discarded which have the following properties:

1 Area less than or equal to 30 pixels (smaller than the smallest object of interest – step 5).
2 Area greater than or equal to 3100 pixels (larger than the largest object of interest – step 6).
3 Mean greylevel value less than or equal to 198 (greylevel value is less than the darkest 'shadow' within the boundaries of any the objects of interest – step 7).

The output of this procedure frequently assigns more than one region to a single object of interest. So all the regions are merged that are connected and another iteration performed of labelling by connected components (step 8). The region properties of the components are also computed. All components with the following properties are discarded from the output of the connected components routine:

1 Area less than or equal to 175 pixels (area smaller than the smallest object of interest – step 9).

2 Mean greylevel less than or equal to 204 (step 10).
3 Area greater than, less than or equal to 3155 pixels (step 11 – area larger than the largest object of interest).

This iteration eliminates some of the objects of interest that were merged into a large background component. In order to detect these objects, the greylevel image is thresholded at a threshold value of 205 (step 12), conditioned by opening with a disc of radius 3 (step 13), labelled by performing connected components analysis on the output of the opening and the region properties computed for each of the components (step 14). All components are discarded that have a circularity measure higher than a threshold value of 4.4 (step 15) and are smaller than 230 pixels in area (step 16). The outputs of the two procedures are then combined using a logical ⟨OR⟩ operation (step 17). The combined output is conditioned by first closing with a disc of radius 7 and then dilating with a disc of radius 3 (step 18). The boundary pixels of the output of the dilation are shown in Fig. 10 (step 19).

The overall algorithm is described in compact notation as follows:

1 $G^1 = G^0 \bullet disc(5)$
2 $B^2 = fedg(G^1, 3, 9, 10.00, 0.70)$
3 $B^3 = G^0 \geqslant 115$
4 $R^4 = rgg(G^0, (B^2 \cup B^3), 0.001)$
5 $C^5 = size(R^4) \leqslant 30$
6 $C^6 = size(C^5) \geqslant 3100$
7 $C^7 = mg(C^6) \leqslant 198$
8 $C^8 = conn(merge(C^7))$
9 $C^9 = size(C^8) \leqslant 175$
10 $C^{10} = mg(C^9) \leqslant 204$
11 $C^{11} = size(C^{10}) \geqslant 3155$
12 $B^{12} = G^0 \leqslant 205$
13 $B^{13} = B^{12} \circ disc(3)$
14 $C^{14} = conn(B^{13})$
15 $C^{15} = circul(C^{14}) \geqslant 4.4$
16 $C^{16} = size(C^{15}) \leqslant 230$
17 $B^{17} = (C^{16} \leqslant 0) \cup (C^{11} \leqslant 0)$
18 $B^{18} = (B^{17} \bullet disc(7)) \oplus disc(3)$
19 $B^{19} = mark(B^{18})$

Comparing the desired output of the procedure given in Fig. 7 to that obtained by the procedure described above (Fig. 10), the following observations can be made:

1 There are some spurious detections of boundaries where no such boundaries exist on the reference image. The greylevel characteristics of these regions are very similar to those of the objects of interest.
2 The U-shaped object boundary has been detected fairly accurately. How-

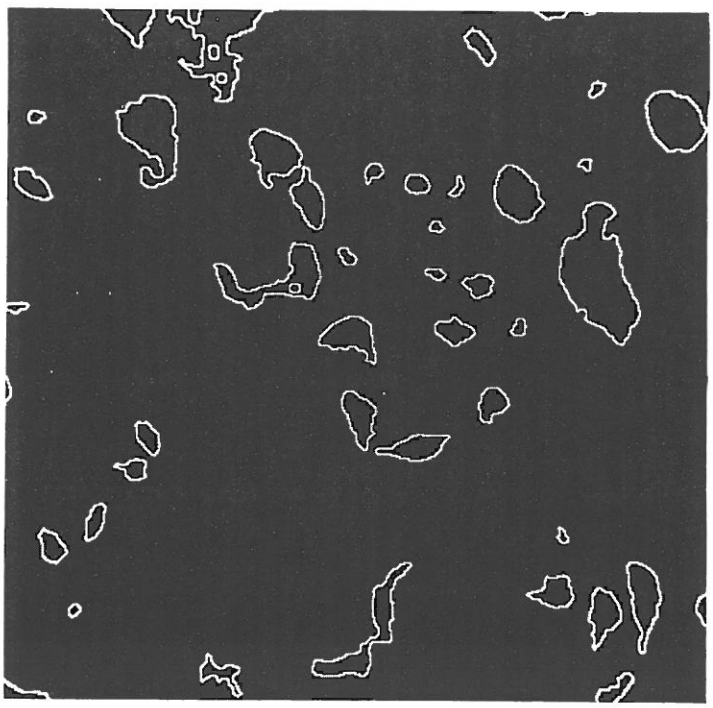

Fig. 10. Image 4. Result of edge detection procedure preserving connectivity.

ever, the region growing algorithm has not defined the boundary of the large object at the top edge of the image well. This is a consequence of our choosing the facet edge detector parameters in order to preserve the connectivity of the two parts of the U-shaped object. If this were not a concern, an alternate procedure could be applied that directly processes the output of a thresholding procedure on the original greylevel image. This is then followed by conditioning using morphology and some connected components analysis to produce the image of Fig. 11. It is apparent that some of the same spurious detections that were present in the more complicated procedure described previously are still present in the thresholding based procedure. However, the boundary of the large object on the top edge is much better defined and the U-shaped object has now become disconnected into two distinct objects. Clearly, the greylevel characteristics of the U-shaped object are not the only factors used by the expert who generated the true delineation of the objects. Using just the greylevel information, it is impossible to preserve simultaneously the fidelity of the boundaries of the U-shaped and the large objects. Clearly, this suggests the need for some higher level knowledge of the nature of the objects of the scene which can then be used to delineate object boundaries. Knowledge about the content of the scene could also be used

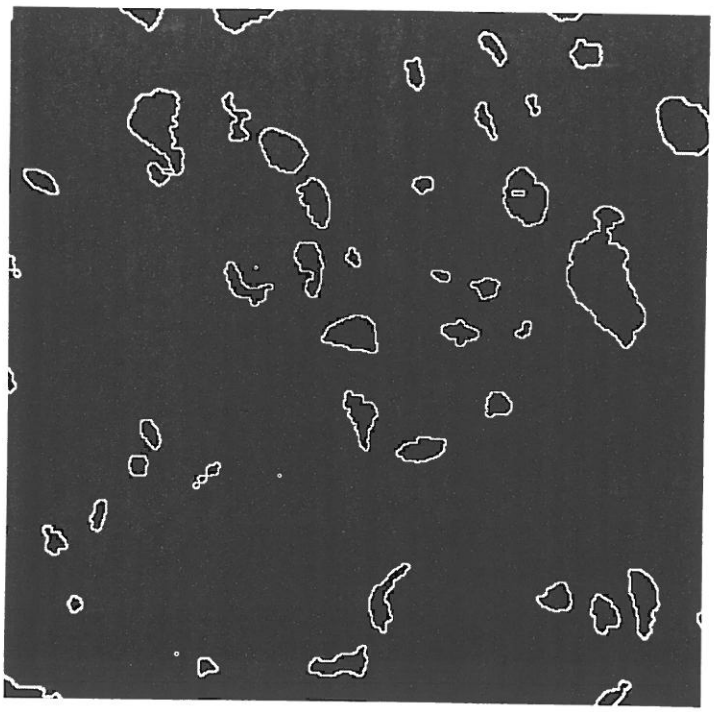

Fig. 11. Image 4. Result of edge detection procedure not preserving connectivity.

to eliminate spurious detections that occur in physically impossible locations.

Conclusions

Edge detection procedures have been applied to four microscope images: one confocal and three conventional images. Three powerful image processing techniques have been used – thresholding, mathematical morphology and facet edge detection. Boundary delineations have been obtained by iterations of conditioning and labelling operations. The boundary delineation procedures combine the output of different edge detection techniques so as to obtain the best possible result relative to the ideal boundary. The trade-offs involved in the design of edge detection procedures have been described. In some instances it is impossible to design an image analysis procedure that uses only greylevel information to perform a boundary detection that is similar to that performed by a human expert. The procedures presented had parameters that depended on the scale and brightness of both the objects of interest and the extraneous objects. This information will have to be supplied by a higher level module that has some *a priori* knowledge of these parameters in a complete system for boundary delineation in cell imagery.

References

Costa, M. (1990). *A Practical Guide to Task-oriented Sequences of Morphological Operations for use in Image Analysis*. Technical Report EE-ISL-90-01, Intelligent Systems Laboratory, Department of Electrical Engineering, University of Washington, Seattle WA.

Garbay, C. (1986). Image structure representation and processing: a discussion of some segmentation methods in cytology. *IEEE Transactions on Pattern Analysis and Machine Intelligence*, **PAMI-8**.

Giardina, C. R. & Dougherty, E. D. (1988). *Morphological Methods in Image and Signal Processing*. Englewood Cliffs, NJ: Prentice Hall.

Haralick, R. M. (1984). Digital step edges from zero crossings of second directional derivatives. *IEEE Transactions on Pattern Analysis and Machine Intelligence*, **PAMI-6**.

Haralick, R. M. & Shapiro, L. G. (1991). *Computer and Robot Vision*. Reading, MA: Addison-Wesley.

Haralick, R. M., Strenberg, S. R. & Zhuang, X. (1987). Image analysis using mathematical morphology. *IEEE Transactions on Pattern Analysis and Machine Intelligence*, **PAMI-9**.

Joo, H. (1991). *Towards the Automatic Generation of Mathematical Morphology Procedures using Predicate Logic*. PhD thesis, University of Washington, Seattle WA.

Lumia, R. L., Shapiro, L. G. & Zuniga, O. (1983). A new connected components algorithm for virtual memory computers. *Computer Vision, Graphics and Image Processing*, **22**.

Prewitt, J. (1970). Object enhancement and extraction. In *Picture Processing and Psychopictorics*, ed. B. Lipkin & A. Rosenfeld. New York: Academic Press.

Rosenfeld, A. & Kak, A. (1982). *Digital Picture Processing*. New York: Academic Press.